Journal Pre-proof

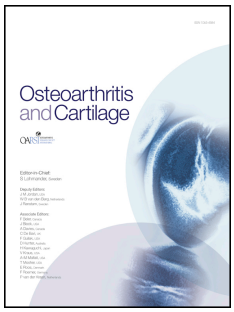

Crucial role of the terminal complement complex in chondrocyte death and hypertrophy after cartilage trauma

Jana Riegger, Markus Huber-Lang, Rolf E. Brenner

PII: S1063-4584(20)30027-3

DOI: https://doi.org/10.1016/j.joca.2020.01.004

Reference: YJOCA 4581

To appear in: *Osteoarthritis and Cartilage*

Received Date: 31 May 2019

Revised Date: 9 January 2020

Accepted Date: 10 January 2020

Please cite this article as: Riegger J, Huber-Lang M, Brenner RE, Crucial role of the terminal complement complex in chondrocyte death and hypertrophy after cartilage trauma, *Osteoarthritis and Cartilage*, https://doi.org/10.1016/j.joca.2020.01.004.

Crucial role of the terminal complement complex in chondrocyte death and hypertrophy after cartilage trauma

Authors: Jana Riegger [1], Markus Huber-Lang [2] and Rolf E. Brenner [1]

[1] Division for Biochemistry of Joint and Connective Tissue Diseases, Department of Orthopedics, University of Ulm, Ulm, Germany

[2] Institute of Clinical and Experimental Trauma-Immunology, University Hospital of Ulm, Ulm, Germany

Abstract

Objective: Innate immune response and particularly terminal complement complex (TCC) deposition are thought to be involved in the pathogenesis of posttraumatic osteoarthritis. However, the possible role of TCC in regulated cell death as well as chondrocyte hypertrophy and senescence has not been unraveled so far and was first addressed using an ex vivo human cartilage trauma-model.

Design: Cartilage explants were subjected to blunt impact (0.59 J) and exposed to human serum (HS) and cartilage homogenate (HG) with or without different potential therapeutics: RIPK1-inhibitor Necrostatin-1 (Nec), caspase-inhibitor zVAD, antioxidant N-acetyl cysteine (NAC) and TCC-inhibitors aurintricarboxylic acid (ATA) and clusterin (CLU). Cell death and hypertrophy/ senescence-associated markers were evaluated on mRNA and protein level.

Results: Addition of HS resulted in significantly enhanced TCC deposition on chondrocytes and decrease of cell viability after trauma. This effect was potentiated by HG and was associated with expression of RIPK3, MLKL and CASP8. Cytotoxicity of HS could be prevented by heat-inactivation or specific inhibitors, whereby combination of Nec and zVAD as well as ATA exhibited highest cell protection.

Conclusions: Our findings imply crucial involvement of the complement system and primarily TCC in regulated cell death and phenotypic changes of chondrocytes after cartilage trauma. Inhibition of TCC formation or downstream signaling largely modified serum-induced pathophysiologic effects and might therefore represent a therapeutic target to maintain the survival and chondrogenic character of cartilage cells.

Keywords: Cartilage trauma; terminal complement complex; Aurintricarboxylic acid; Regulated cell death; Hypertrophy; Senescence

Introduction

The complement system represents a major effector of the innate immunity and plays a crucial role in trauma response [1]. Complement activation finally leads to the formation of the terminal complement complex (TCC), comprising the complement factors C5b, C6, C7, C8 and C9 (C5b-9), which incorporates into the cell membrane, mediating cell death and, in sublytic amounts, further pathophysiological processes including inflammation [2-4]. It has been shown that the soluble form of the TCC (sTCC) and other components of the complement system, such as anaphylatoxins and C3bBbP (the C3 convertase of the alternative pathway), are enhanced in synovial fluids of patients after knee injury or suffering from osteoarthritic (OA) disease, implying complement activation (**compare Fig. 1**) [5, 6].

Trauma-related activation of the complement cascade and subsequent TCC formation is thought to be triggered by damage-associated molecular patterns (DAMPs), released after tissue injury [7]. In regard to cartilage trauma, extracellular matrix components like fibromodulin or cartilage oligomeric matrix protein,[5] as well as intracellular high mobility group box 1 (HMGB1) [4, 8], are not only linked to the pathogenesis of OA disease but also represent typical inducers of the complement cascade [9-11]. Indeed, we previously observed enhanced TCC deposition on the membrane of chondrocytes after blunt cartilage trauma in a rabbit *in vivo* model, which was further increased by concurrent intraarticular bleeding (hemarthrosis) [12]. Moreover, blood exposure potentiated trauma-related cell death as well as catabolic and pro-inflammatory processes after *ex vivo* traumatization of human cartilage explants[12], indicating additive effects of cartilage trauma and serum components. In line with that, Wang *et al.* described some cytotoxic effects after excessive C5b-9 deposition, while sublytic concentrations induced the gene expression of several

mediators, such as matrix metalloproteinases (MMPs) and chemokines, known to be associated with osteoarthritis, consequent chondrocyte hypertrophy and senescence [5, 13, 14]. Although, these findings imply an involvement of the TCC in the development of OA disease, and in particular posttraumatic OA (PTOA), the specific complement-mediated pathomechanism remains unclear.

Besides the catabolic and pro-inflammatory response, C5b-9 has been found to influence cell fate, ranging from pro-survival signaling up to different modalities of regulated cell death [15-17]. In fact, Lusthaus *et al.* identified receptor-interacting protein kinase 1 (RIPK1) and 3 (RIPK3), and mixed-lineage kinase domain-like protein (MLKL) as important regulators in complement-induced cell death in human cell lines [15], indicating that C5b-9 might lead to necroptosis, which we recently evidenced in human OA cartilage [18]. The necroptotic signaling pathway usually depends on activation of death receptors and the absence of caspase 8 (CASP8), which enables RIPK1 phosphorylation and its interaction with RIPK3, forming the necrosome [19]. Subsequent phosphorylation of MLKL initializes the oligomerization of the protein and incorporation into the plasma membrane. The resulting ion influx results in the rupture of the plasma membrane and release of DAMPs triggering an inflammatory response, wherefore necroptosis is considered as “dirty” mode of regulated cell death [20].

Thus, we proposed that the TCC not only causes cartilage-destructive effects, but also promotes regulated cell death as well as phenotypical change of the surviving chondrocytes after cartilage trauma. In the following, we addressed this hypothesis in a human *ex vivo* cartilage trauma-model and provide first evidence of complement-mediated cell death and senescence of the affected cartilage cells. In order to clarify and alleviate the potentially detrimental mechanisms of serum exposition, different therapeutic approaches were tested – the antioxidant N-acetylcysteine (NAC), pan-

caspase inhibitor z-VAD-FMK (zVAD) and RIP1 inhibitor necrostatin 1 (Nec) as well as aurintricarboxylic acid (ATA) [21] and clusterin (CLU) as inhibitors of TCC formation.

Methods

Specimen preparation and cultivation conditions: Human cartilage was obtained from donors undergoing total knee joint replacement due to OA. Informed consent was obtained from patients according to the terms of the Ethics Committee of the University of Ulm (ethical approval number 353/18). Overall, macroscopically intact tissue (International Cartilage Repair Society (ICRS) [22] score ≤1) from 20 patients (mean age 63 years, ranging 48-82 years) as well as highly degenerated tissue (ICRS ≥3) from 8 patients (mean age 63 years, ranging 54-75 years), was included in the study. Full-thickness cartilage explants (Ø= 6 mm) were harvested and cultivated in serum-containing medium (Supplementary material S1) for at least 24h at 37℃, 5% CO_2 and 95% humidity. Afterwards, the explants were traumatized and cultivated in serum-free medium (Supplementary material S1). Highly degenerated tissue was immediately fixed and cryo-conserved, respectively, without cultivation. Detailed information about the sample allocation is provided as supplementary material **S2.**

Impact loading and subsequent treatment: Cartilage explants were subjected to a defined impact energy of 0.59 J by using a drop-tower model as previously described [23, 24]. Unimpacted explants served as controls. Impacted/unimpacted cartilage explants were stimulated with 10%-20% (v/v) pooled human serum (HS; Innovative Research, Novi, MI, USA) with and without homogenized cartilage (HG; 20 µg/mL) and treated with 2 mM NAC (Sigma), 40 µM Nec-1 (Sigma), 2.5 µM

necrosulfonamide (NSA; Tocris Bioscience, Bristol, UK), 20 µM zVAD (R&D Systems, Wiesbaden, Germany), 75 µg/mL ATA (Sigma) or 30 µg/mL CLU (R&D Systems) for 4 days. Fresh additives were provided after 24 h.

Immunohistochemical (IHC) analysis: For IHC, paraffin-embedded sections (3.5 µm) were dewaxed and rehydrated. Antigen retrieval was performed by incubation in sodium citrate buffer pH 6.0 at 65 ℃ overnight. Un specific antigens were blocked with the DAKO blocking reagent (Dako, Glostrup, Denmark), followed by overnight incubation with primary antibody against human C5b-9 (Quidel, San Diego, CA, USA, 1:250 diluted), CASP8 (ab25901, abcam, Cambridge, UK, 1:500 diluted), cleaved CASP8 (NB100-56116; NOVUS Biologicals, Centennial, CO, USA), p-MLKL ([EPR9514] phospho S358; abcam, Cambridge, UK) or RIPK3 (GTX107574; GeneTex, Irvine, CA, USA, 1:250 diluted) at 4℃. Se ctions were treated with 3% hydrogen peroxide before starting the staining with the Dako LSAB2 System-HRP kit (Dako, Glostrup, Denmark). In all samples a final staining of cell nuclei by Gill's hematoxylin No 3 (Sigma) was performed.

Live/Dead Cell Cytotoxity Assay: To determine the percentage of viable cells, a Live/Dead® Viability/Cytotoxity Assay (Molecular Probes, Invitrogen, Darmstadt, Germany) was performed as previously described [24]. In short, unfixed tissue sections (0.5 mm thickness) were stained with 1 µM calcein AM and 2 µM ethidium homodimer-1 for 30 minutes. After washing in PBS, they were microscopically analyzed by means of a z-stack module (software AxioVision, Carl Zeiss, Jena, Germany).

mRNA Isolation and cDNA Synthesis: For total RNA isolation, cryopreserved cartilage explants were pulverized with a microdismembrator S (B. Braun Biotech, Melsungen, Germany). Subsequently, RNA was isolated using the Lipid Tissue Mini Kit (Qiagen, Hilden, Germany). RNA was reverse transcribed with the Omniscript RT Kit (Qiagen) and used for quantitative real-time PCR-analysis (StepOnePlus™ Real-Time PCR System, Applied Biosystems, Darmstadt, Germany).

Quantitative Real-Time Polymerase Chain Reaction (qRT-PCR): Determination of the relative expression levels was performed by means of qRT-PCR analysis ($2^{-\Delta\Delta Ct}$ method). To detect desired sequences, TaqMan® Gene Expression Master Mix for TaqMan® Gene Expression Assay (both Applied Biosystems) was used for probes listed in supplementary material S1. Additionally, Power SYBR® Green PCR Master Mix (Applied Biosystems) was used for 18S rRNA, 5'-CGCAGCTAGGAATAATGGAATAGG-3' (forward) and 5'-CATGGCCTCAGTTCCGAAA-3' (reverse), and Platinum® SYBR® Green qPCR SuperMix-UDG (Invitrogen) for GAPDH, 5'-TGGTATCGTGGAAGGACTCATG-3' (forward) and 5'-TCTTCTGGGTGGCAGTGATG-3' (reverse). Target mRNA-expression was normalised to the endogenous controls 18S rRNA, GAPDH and HPRT1.

CH-50 Assay - Complement hemolytic serum activity: Hemolytic activity of HS in the absence and presence of the ATA, CLU, NAC, Nec or zVAD was assessed as previously described [25]. Briefly, sheep erythrocytes (Oxoid, Wesel, Germany) were sensitized with hemolysin (Colorado Serum Company, Denver, CO) and exposed to dilutions of serum samples in TBS (pH 7.35, 37℃, 60 min). The complement reaction was stopped by the addition of ice-cold TBS followed by a centrifugation step (700 x

g, 5 min). Absorption values of the supernatant fluids were determined by spectrophotometry at 541 nm. The complement hemolytic serum activity (CH-50) defines the exact serum concentration that results in complement-mediated lysis of 50% of sensitized sheep erythrocytes.

Chondrocyte isolation: Chondrocytes were enzymatically isolated from macroscopically intact human cartilage of 7 patients (mean age 69, range 56-82 years). In short, full-thickness cartilage was minced and digested for 45 min with 0.2 % pronase (Sigma) and overnight with 0.025 % collagenase (Sigma). After washing with PBS and filtration through a 40 µm cell strainer (BD GmbH), cells (passage 0) were cultured in serum-containing chondrocyte medium (see above). Chondrocytes were split at a confluence of 80 % and used at passage 1 to 3.

C5b-9 cell-ELISA: Quantification of membrane-bound C5b-9 on the cell surface of isolated chondrocytes was performed in 96-well culture plates (protocol adopted from Jeon et al. [26]). In short, 6,000 cells/well were seeded and cultivated overnight. Cells were stimulated with 20% HS (v/v) with and without HG (20 µg/mL) at 37 ℃ for 2 h. Afterwards, cells were fixed with 4% paraformaldehyde (15 min) and incubated in blocking buffer (5% bovine serum albumin, Sigma) for 1 h at 37 ℃, before incubation with a rabbit polyclonal C5b-9 antibody (abcam) diluted 1:4000 at 37 ℃ for 2 h. After incubation with an HRP-conjugated anti-rabbit IgG (1:10000; Sigma) for 1 h, 3,3′,5,5′-tetramethylbenzidine (TMB, Sigma) was added and the absorbance was measured at 450 nm. Data values were normalized to the DNA content of the cells, determined by subsequent Hoechst staining.

Senescence-associated (SA)-β-galactosidase (gal) staining: SA-β-gal staining was done using a SA-β-gal staining kit according to the manufacturer's protocol (Cell Signaling Technology, Danvers, MA, USA). In short, cells were seeded on cover slides (15.000 cells/ cm^2) and cultivated overnight. Cells were stimulated as described in the figure legends for 24 h fixed in a 2% formaldehyde and 0.2% glutaraldehyde solution for 15 minutes. After washing with PBS, cells were stained overnight in an X-gal staining solution at 37℃.

Statistical Analyses: Experiments were analyzed by using GraphPad Prism version 8.1.1 (GraphPad Software). Data sets with n ≥ 5 were tested for outliers with the Grubbs outlier test. Outliers were not included in statistical analyses. For parametric data sets, a 1-way analysis of variance (ANOVA) with Bonferroni posttest was used. In case the gene expression ratio for CLU and CD59, respectively (figure 2E), statistical analysis was performed by an unpaired multiple t test. Data values are depicted as boxplots (median; whiskers: min to max) and in case of the CH-50 assay (figure 4B) as bars (mean with SD). The significant level was set to α= .05.

Results

TCC deposition and chondrocyte defense in OA cartilage and ex vivo

IHC staining of C5b-9 in highly degenerated cartilage (ICRS grade ≥3; **Fig. 2A**) revealed increased TCC deposition on chondrocytes, as compared to macroscopically intact tissue (ICRS grade ≤ 1; **Fig. 2B**). TCC-positive cells were mainly located in proximity to the surface of the cartilage, gradually diminishing towards the lower layers (**Supplementary material S3**). The same allocation could

be found for cleaved CASP8 and RIPK3 positive cells, while p-MLKL was predominantly associated to the middle and lower zones (**Supplementary material S3).** *Ex vivo* traumatization and serum exposition of macroscopically intact tissue resulted in high TCC deposition which was evenly distributed over the entire explant (**Fig. 2C)**, which corresponded to the expression of apoptosis- and necroptosis-associated proteins (Supplementary material **S4**).

Moreover, the gene expression of the endogenous complement regulators CD59 and CLU were significantly enhanced in highly degenerated cartilage ([vs C] CD59: 2.6-fold, p = 0.012; CLU: 4.2-fold, p≤ 0.0001; **Fig. 2E**). Equivalent cellular defense towards the C5b-9 complex could be observed after e*x vivo* exposition towards HS and was found to arise in a concentration-dependent manner (**Fig. 2F, G**).

Serum exposure and cartilage trauma have additional effect on cell death

Cell viability was significantly decreased after cartilage trauma ([vs C] -20.8%; p ≤ 0.0001, **Fig. 3A**). Addition of HS enhanced trauma-related cell death in a concentration-dependent manner. Furthermore, decrease in cell viability was highly associated with the gene expression of necroptotic markers ([vs C] RIPK3: 2.3-fold, p = 0.007; MLKL: 1.7-fold, P = 0.0007).

Interestingly, serum exposure had no significant effect on cell viability and gene expression of apoptosis and necroptosis markers in unimpacted cartilage, implying additive effects between HS and preceding blunt trauma, as also shown for gene expression of CD59.

Stimulation with heat-inactivated HS had no significant effect on the gene expression of cell death-associated markers and complement regulators, respectively.

TCC deposition on isolated chondrocytes is enhanced by DAMPs and can be alleviated by ATA or CLU

To investigate potential triggers and inhibitors of TCC formation, membrane-bound C5b-9 was determined by a specific cell ELISA, allowing relative quantification of TCC deposition on the cell surface.

Addition of HS (20% v/v) lead to a 1.8-fold increase of the relative TCC deposition as compared to cells incubated under serum-free conditions (**Fig. 4A**). Addition of trauma-conditioned medium (TCM), obtained 24h after trauma from untreated traumatized cartilage explants, or addition of cartilage homogenate (HG) further enhanced the amounts of membrane-bound C5b-9, leading to a 2.6-fold and 2.8-fold increase, respectively. Heat-inactivation of the HS, as well as addition of TCC-inhibitors ATA and CLU significantly prevented TCC deposition on the surface of chondrocytes ([vs HS+HG] ATA: -1-fold, $p = 0.004$; CLU: -1.2-fold, $p = 0.0004$).

Furthermore, hemolytic activity of the HS and potential inhibition of the therpeutics was evaluated by means of a CH-50 assay (**Fig. 4B**). While addition of NAC, Nec-1 or zVAD had no significant effect on TCC formation and the CH-50 values, respectively, TCC-inhibitors ATA or CLU considerably decreased hemolytic activity of the HS, which approximately reached the zero value (TBS control).

Complement-mediated cytotoxicity can be prevented by inhibition of regulated cell death or TCC formation

Serum-mediated cell death was further enhanced after addition of cartilage homogenate ([vs T+30%HS] -7.7%), which itself had no cytotoxic effect after trauma (**Fig. 5A**). Compared to T+30%HS+HG, cell viability was largely maintained by

treatment with TCC-inhibitors ATA or CLU as well as NAC, Nec, zVAD or NSA. Additive cell protective effects were observed after combining Nec and zVAD. Heat-inactivated HS revealed rather beneficial effects regarding the cell viability.

In line with the results of the live dead assay, gene expression of apoptotic and necroptotic markers was significantly enhanced after stimulation with HS and HG ([vs C] CASP8: 1.7-fold, p = 0003; RIPK3: 2.3-fold, p = 0.0002; MLKL: 1.9-fold, p ≤ 0.0001) (**Fig. 5C, D, F**). Gene expression levels of RIPK1 and CASP3 were not found to be significantly increased (**Fig. 5B, E**).

While monotherapeutic application of Nec suppressed serum-mediated gene expression of RIPK3 by 1.6-fold (p = 0.047), MLKL by 1.6-fold (p = 0.0003) and CASP8 by 1.5-fold (p = 0.026), the combined treatment with zVAD exhibited additive effects and attenuated mRNA levels of RIPK3 by 1.8-fold (p = 0.028), MLKL by 2.2-fold (p ≤ 0.0001) and CASP8 by 2-fold (p = 0.0006). Treatment with ATA, NAC and zVAD, resulted in significant effects only in the case of MLKL (ATA: 1.8-fold, p ≤ 0.0001; NAC: 1.4-fold, p = 0.0033; zVAD: 1.6-fold, p = 0.0008). TCC-inhibitor CLU significantly suppressed the gene expression of RIPK3 by 2.8-fold (p = 0.0006), though, had no effect on that of MLKL.

Overall, ATA exhibited higher cell protective effects as compared to CLU in the tested concentrations, which was in line with mRNA levels of MLKL.

Serum exposition promotes gene expression of hypertrophic and senescence markers

To investigate the influence of HS on the phenotype of the surviving chondrocytes after cartilage trauma, gene expression of different markers associated with chondrocyte hypertrophy and/ or senescence was evaluated (**Fig. 6A-F**).

Even without preceding traumatization, stimulation with HS and HG increased mean mRNA levels of COL10A1 (2.7-fold; p = 0.395), MMP-13 (3.1-fold; p = 0.115), CXCL1 (17.5-fold; p = 0.81), IL-8 (18.7-fold; p = 0.964), VEGFA (2.1-fold; p = 0.083) and RUNX2 (7.9-fold; p = 0.002), though this was only statistically significant in case of RUNX2. As compared to cartilage trauma alone, additional stimulation with HS (30%) and HG further enhanced the gene expression of COL10A1 by 2.7-fold, MMP-13 by 2.4-fold, CXCL1 by 45.6-fold (p = 0.002), IL-8 by 54-fold (p = 0.02), RUNX2 by 5.8-fold (p = 0.0034) and VEGFA by 1.7-fold (p= 0.047). These effects were alleviated by the therapeutic approaches to different degrees, though zVAD exclusively attenuated the gene expression of COL10A1. Overall, CLU had stronger anti-hypertrophic effects as compared to ATA.

Serum exposition leads to secretion of SASP markers and enhanced SA-ß-gal staining

Trauma- and serum-related secretion of senescence-associated secretory phenotype (SASP) markers MMP-13 and IL-6 into the culture medium was determined by specific ELISAs (**Fig. 7A, B**).

Serum exposition enhanced trauma-induced secretion of MMP-13 by about 141 pg/mL (p = 0.37) and IL-6 by about 10 pg/mL (p = 0.0012). Release of MMP-13 was significantly suppressed by treatment with NAC (-206 pg/mL), Nec (-291 pg/mL,) and CLU (-173 pg/mL).

In contrast to the secretion of MMP-13, additive effects of Nec and zVAD were found regarding the release of IL-6 which was reduced by 13 ng/mL (p ≤ 0.0001). It should be noted that the serum-levels of MMP-13 and IL-6 were below the detection limit of the ELISAs (MMP-13: 6 pg/mL; IL-6: 2 pg/mL) at a concentration of 30% (v/v).

Moreover, serum exposition resulted in enhanced SA-β-gal activity in isolated chondrocytes and was associated with morphological changes of the cells, characterized by a roundish shape (**Fig. 7C**). Heat-inactivated HS and/ or stimulation with HG also increased the percentage of SA-β-gal-positive cells, though to a lesser extent (**Fig. 7D**).

Discussion

Complement components and in particular membrane-bound C5b-9 is thought to play a central role in OA progression [5, 12]. In the present study we found evidence of novel aspects in TCC-mediated pathophysiology, comprising regulated cell death as well as phenotypical changes of the surviving chondrocytes in a human *ex vivo* cartilage trauma-model.

Recently, we observed significantly increased incidence of necroptotic cell death in highly degenerated human cartilage tissue [18]. However, necroptotic processes could not be induced by sole *ex vivo* traumatization and required co-stimulation with TNF-a and cycloheximide under serum-free conditions. Of note, all studies addressing necroptosis are either based on special stimulation cocktails (containing i.e. TNF-a, cycloheximide or SMAC mimetics and zVAD) or were investigated *in vivo* [27-29]. In the present approach, including human serum, necroptosis-associated gene expression was significantly increased after *ex vivo* trauma, suggesting that the serum might represent the missing link between mechanical stress and necroptosis. Finally, Lusthaus *et al.* reported clear evidence for C5b-9 mediated necroptotic cell death [15]. Although we observed equal allocation of TCC-, RIPK3-, and CASP8-positive cells in highly degenerated cartilage as well as a concurrent increase of cell death associated markers after *ex vivo* trauma and serum exposition, chondrocytes were

predominantly positive for cleaved CASP8 while insignificant staining was found for p-MLKL.

Moreover, the live dead staining revealed additive effects of trauma and serum exposition, which was enhanced by co-stimulation with cartilage homogenate. Interestingly, HS and HG did not result in significant cytotoxicity in unimpacted cartilage explants, suggesting that a mechanical impact was required for TCC-associated cell death signaling. In accordance with Shi *et al.*, we assume that serum exposition and subsequent TCC deposition might be a crucial parameter in regulated cell death, most likely in a sensitizing manner [3]. Serum- and trauma-induced chondrocyte death could be attenuated by Nec and zVAD – and especially in combined application – indicating that both apoptotic and necroptotic cell death might be involved despite poor staining of p-MLKL. Since cell protective effects of Nec are not limited to its anti-necroptotic features but might also result from inhibition of apoptosis and autophagy [30, 31], an specific MLKL-inhibitor, NSA, was additionally tested and exhibited significant decrease of complement-dependent cytotoxicity. Ziporen *et al.* corroborated that TCC-induced regulated cell death could be alleviated by pan-caspase inhibitor zVAD and concluded that C5b-9 is able to activate two different cell death pathways, one involving caspase-dependent cleavage of Bid and one which is caspase-/ Bid-independent. Moreover, they suggested that Bid might also play a role in regulated necrosis [16], which could refute the common paradigm of the necroptotic pathway. This might explain why we found evidence of both caspase activity and necroptotic markers after trauma and serum exposition. Anyhow, the precise mode of TCC-induced cell death and the underlying mechanisms still remain unclear and, therefore, further analysis are needed.

Regarding the cell protective effects of the TCC-inhibitors, it is striking that ATA treatment was more efficient as compared to CLU, which “only” prevents from C5b-9

formation. ATA, by contrast, not only inhibits C9 polymerization but also generation of the C3 convertase and subsequent formation of alternative pathway C5 convertase by binding Factor D [21]. While CLU exhibits additional antiapoptotic effects, mainly based on the inhibition of the nuclear factor-κB (NF-κB) pathway [32], ATA has been found to attenuate various intracellular signaling pathways, such as activation of activator protein-1 (AP-1) and NF-κB as well as IκB kinase (IKK), extracellular signal-regulated kinase (ERK), and p38 mitogen-activated protein kinase (MAPK) [33], which are also involved in the progression of PTOA [34, 35]. Moreover, previous studies demonstrated that CLU represents an important mediator in cell protection after tissue injury and subsequent oxidative stress [36], and is significantly enhanced in early stages of OA disease [37].

Our results indicate that serum exposition might cause hypertrophy and expression of SASP markers, which did not necessarily depend on preceding traumatization. Under physiological conditions, TCC components C5 and C9 were found to be predominately located in the hypertrophic zone, associated with endochondral bone formation (ossification) – a process which results in chondrocyte apoptosis [38]. Besides the hypertrophic markers type X collagen and MMP-13, ossification is thought to be driven by excessive expression of chemokines CXCL1 and IL-8, [39] as well as VEGFA and RUNX2, the master transcription factor in chondrocyte hypertrophy [40, 41]. Moreover, SA-ß-gal staining confirmed that the phenotypical change of the chondrocytes was not limited to hypertrophy but was also connected to senescence. In fact, cellular senescence has been associated to hypertrophy of fibroblasts [42], but has also been found to be relevant in hypertrophic chondrocytes in OA [43, 44]. In the end, both chondrocyte hypertrophy and senescence are linked to apoptosis in the context of terminal differentiation – thus completing the circle [45].

Interestingly, we found that serum-induced gene expression of IL-8 and RUNX2 could not be prevented by heat-inactivation, implying that other heat-stable serum components might act as a trigger. In fact, our analysis of heat-inactivated HS revealed for example enhanced concentration of anaphylatoxin C5a, which might be generated during the heating process (data not shown). Since C5a has been reported to directly increase the IL-6 and IL-8 secretion in porcine chondrocytes [46], it should be considered that the anaphylatoxin is also somehow involved in our model. However, possible effects of C5a in heat-inactivated serum could not be confirmed in case of IL-6 release, therefore, further experiments addressing the implication of other serum components are required to unravel the respective contribution.

It should be noted that inhibition of caspase-induced apoptosis by zVAD did not attenuate the expression of SASP components, but exhibited additive effects with Nec, which had generally more beneficial effects as compared to zVAD. This corresponds to our recent study that zVAD leads to pro-inflammatory effects after cartilage trauma probably by enhancing necroptotic processes due to CASP8-inhibiton [18]. According to previous findings, Nec reduces chemokine and catabolic enzyme expression by suppression of the JNK/AP-1 and NF-κB signaling pathways [30, 47]. Previously, we reported similar features for the antioxidant NAC after cartilage trauma [24], which also attenuated most of the TCC-induced processes in the present study. In fact, TCC binding has been shown to induce both translocation of NF-kB and activation of different MAPK pathways [2].

Overall, we demonstrated that complement activation and subsequent TCC deposition plays a crucial role in different modes of regulated cell death as well as phenotypical changes of surviving chondrocytes after cartilage trauma (**Fig. 1**). These processes could be attenuated by corresponding upstream and downstream treatment strategies. In this context, we found novel evidence for the connection

between hypertrophy, senescence and apoptosis as central processes related to enchondral ossification and potential involvement of the complement system. Prevention of TCC-mediated pathomechanisms might maintain cartilage integrity and stabilize the chondrogenic phenotype of surviving chondrocytes. Consequently, the complement cascade and in particular the TCC represents a promising therapeutic target.

Acknowledgements: The authors would like to thank Renate Wanner and Bettina Klohs for excellent technical assistance. This study was partly supported by the German Research Foundation (BR 919/12-1 and CRC 1149-A01).

Authors contributions: JR contributed to the acquisition and analysis of the data. REB, MHL and JR contributed to the study design, interpretation of data and were involved in drafting and revising the article critically for important intellectual content. All authors approved the final submitted version and take shared responsibility for the accuracy of the presented data.

Conflict of interest: The authors declare no conflict of interest.

References

1. Huber-Lang M, Lambris JD and Ward PA. Innate immune responses to trauma. *Nat Immunol* 2018;19:327-41.
2. Tegla CA, Cudrici C, Patel S, Trippe R, Rus V, Niculescu F, et al. Membrane attack by complement: the assembly and biology of terminal complement complexes. *Immunol Res* 2011;51:45-60.
3. Shi H, Williams JA, Guo L, Stampoulis D, Francesca Cordeiro M and Moss SE. Exposure to the complement C5b-9 complex sensitizes 661W photoreceptor cells to both apoptosis and necroptosis. *Apoptosis* 2015;20:433-43.

4. Kim SY, Son M, Lee SE, Park IH, Kwak MS, Han M, et al. High-Mobility Group Box 1-Induced Complement Activation Causes Sterile Inflammation. *Front Immunol* 2018;9:705.
5. Wang Q, Rozelle AL, Lepus CM, Scanzello CR, Song JJ, Larsen DM, et al. Identification of a central role for complement in osteoarthritis. *Nat Med* 2011;17:1674-9.
6. Struglics A, Okroj M, Sward P, Frobell R, Saxne T, Lohmander LS, et al. The complement system is activated in synovial fluid from subjects with knee injury and from patients with osteoarthritis. *Arthritis Res Ther* 2016;18.
7. Huber-Lang M, Kovtun A and Ignatius A. The role of complement in trauma and fracture healing. *Semin Immunol* 2013;25:73-8.
8. Liu-Bryan R. Synovium and the innate inflammatory network in osteoarthritis progression. *Curr Rheumatol Rep* 2013;15:323.
9. Sjoberg A, Onnerfjord P, Morgelin M, Heinegard D and Blom AM. The extracellular matrix and inflammation: fibromodulin activates the classical pathway of complement by directly binding C1q. *J Biol Chem* 2005;280:32301-8.
10. Happonen KE, Saxne T, Aspberg A, Morgelin M, Heinegard D and Blom AM. Regulation of complement by cartilage oligomeric matrix protein allows for a novel molecular diagnostic principle in rheumatoid arthritis. *Arthritis Rheum* 2010;62:3574-83.
11. Ke X, Jin G, Yang Y, Cao X, Fang R, Feng X, et al. Synovial Fluid HMGB-1 Levels are Associated with Osteoarthritis Severity. *Clin Lab* 2015;61:809-18.
12. Joos H, Leucht F, Riegger J, Hogrefe C, Fiedler J, Durselen L, et al. Differential Interactive Effects of Cartilage Traumatization and Blood Exposure In Vitro and In Vivo. *Am J Sports Med* 2015;43:2822-32.
13. Lotz M and Loeser RF. Effects of aging on articular cartilage homeostasis. *Bone* 2012;51:241-8.
14. Bao XN and Hu XY. Up-regulated expression of E2F2 is necessary for p16INK4a-induced cartilage injury. *Bmc Musculoskel Dis* 2018;19.
15. Lusthaus M, Mazkereth N, Donin N and Fishelson Z. Receptor-Interacting Protein Kinases 1 and 3, and Mixed Lineage Kinase Domain-Like Protein Are Activated by Sublytic Complement and Participate in Complement-Dependent Cytotoxicity. *Front Immunol* 2018;9:306.
16. Ziporen L, Donin N, Shmushkovich T, Gross A and Fishelson Z. Programmed necrotic cell death induced by complement involves a Bid-dependent pathway. *J Immunol* 2009;182:515-21.
17. Silawal S, Triebel J, Bertsch T and Schulze-Tanzil G. Osteoarthritis and the Complement Cascade. *Clin Med Insights Arthritis Musculoskelet Disord* 2018;11:1179544117751430.
18. Riegger J and Brenner RE. Evidence of necroptosis in osteoarthritic disease: investigation of blunt mechanical impact as possible trigger in regulated necrosis. *Cell Death Dis* 2019;10:683.
19. Vanden Berghe T, Linkermann A, Jouan-Lanhouet S, Walczak H and Vandenabeele P. Regulated necrosis: the expanding network of non-apoptotic cell death pathways. *Nat Rev Mol Cell Biol* 2014;15:135-47.
20. Heckmann BL, Tummers B and Green DR. Crashing the computer: apoptosis vs. necroptosis in neuroinflammation. *Cell Death Differ* 2019;26:41-52.
21. Lee M, Guo JP, McGeer EG and McGeer PL. Aurin tricarboxylic acid self-protects by inhibiting aberrant complement activation at the C3 convertase and C9 binding stages. *Neurobiol Aging* 2013;34:1451-61.

22. Kleemann RU, Krocker D, Cedraro A, Tuischer J and Duda GN. Altered cartilage mechanics and histology in knee osteoarthritis: relation to clinical assessment (ICRS Grade). *Osteoarthritis and cartilage / OARS, Osteoarthritis Research Society* 2005;13:958-63.
23. Joos H, Hogrefe C, Rieger L, Durselen L, Ignatius A and Brenner RE. Single impact trauma in human early-stage osteoarthritic cartilage: implication of prostaglandin D2 but no additive effect of IL-1beta on cell survival. *Int J Mol Med* 2011;28:271-7.
24. Riegger J, Joos H, Palm HG, Friemert B, Reichel H, Ignatius A, et al. Antioxidative therapy in an ex vivo human cartilage trauma-model: attenuation of trauma-induced cell loss and ECM-destructive enzymes by N-acetyl cysteine. *Osteoarthritis Cartilage* 2016;24:2171-80.
25. van Dijk H, Rademaker PM and Willers JM. Estimation of classical pathway of mouse complement activity by use of sensitized rabbit erythrocytes. *J Immunol Methods* 1980;39:257-68.
26. Jeon H, Lee JS, Yoo S and Lee MS. Quantification of complement system activation by measuring C5b-9 cell surface deposition using a cell-ELISA technique. *J Immunol Methods* 2014;415:57-62.
27. McComb S, Aguade-Gorgorio J, Harder L, Marovca B, Cario G, Eckert C, et al. Activation of concurrent apoptosis and necroptosis by SMAC mimetics for the treatment of refractory and relapsed ALL. *Sci Transl Med* 2016;8.
28. Lee SW, Rho JH, Lee SY, Kim JH, Cheong JH, Kim HY, et al. Leptin protects rat articular chondrocytes from cytotoxicity induced by TNF-alpha in the presence of cyclohexamide. *Osteoarthritis Cartilage* 2015;23:2269-78.
29. Zhang C, Lin S, Li T, Jiang Y, Huang Z, Wen J, et al. Mechanical force-mediated pathological cartilage thinning is regulated by necroptosis and apoptosis. *Osteoarthritis Cartilage* 2017;25:1324-34.
30. Liang S, Lv ZT, Zhang JM, Wang YT, Dong YH, Wang ZG, et al. Necrostatin-1 Attenuates Trauma-Induced Mouse Osteoarthritis and IL-1 beta Induced Apoptosis via HMGB1/TLR4/SDF-1 in Primary Mouse Chondrocytes. *Front Pharmacol* 2018;9.
31. Wang YQ, Wang L, Zhang MY, Wang T, Bao HJ, Liu WL, et al. Necrostatin-1 Suppresses Autophagy and Apoptosis in Mice Traumatic Brain Injury Model. *Neurochem Res* 2012;37:1849-58.
32. Liu GD, Zhang HM, Hao FY, Hao J, Pan LX, Zhao Q, et al. Clusterin Reduces Cold Ischemia-Reperfusion Injury in Heart Transplantation Through Regulation of NF-kappa B Signaling and Bax/Bcl-xL Expression. *Cell Physiol Biochem* 2018;45:1003-12.
33. Tsi CJ, Chao Y, Chen CW and Lin WW. Aurintricarboxylic acid protects against cell death caused by lipopolysaccharide in macrophages by decreasing inducible nitric-oxide synthase induction via IkappaB kinase, extracellular signal-regulated kinase, and p38 mitogen-activated protein kinase inhibition. *Mol Pharmacol* 2002;62:90-101.
34. Ding L, Heying E, Nicholson N, Stroud NJ, Homandberg GA, Buckwalter JA, et al. Mechanical impact induces cartilage degradation via mitogen activated protein kinases. *Osteoarthritis Cartilage* 2010;18:1509-17.
35. Yan H, Duan X, Pan H, Holguin N, Rai MF, Akk A, et al. Suppression of NF-kappa B activity via nanoparticle-based siRNA delivery alters early cartilage responses to injury. *P Natl Acad Sci USA* 2016;113:E6199-E208.
36. Schwochau GB, Nath KA and Rosenberg ME. Clusterin protects against oxidative stress in vitro through aggregative and nonaggregative properties. *Kidney Int* 1998;53:1647-53.

37. Connor JR, Kumar S, Sathe G, Mooney J, O'Brien SP, Mui P, et al. Clusterin expression in adult human normal and osteoarthritic articular cartilage. *Osteoarthritis Cartilage* 2001;9:727-37.
38. Andrades JA, Nimni ME, Becerra J, Eisenstein R, Davis M and Sorgente N. Complement proteins are present in developing endochondral bone and may mediate cartilage cell death and vascularization. *Exp Cell Res* 1996;227:208-13.
39. Merz D, Liu R, Johnson K and Terkeltaub R. IL-8/CXCL8 and growth-related oncogene alpha/CXCL1 induce chondrocyte hypertrophic differentiation. *J Immunol* 2003;171:4406-15.
40. Ludin A, Sela JJ, Schroeder A, Samuni Y, Nitzan DW and Amir G. Injection of vascular endothelial growth factor into knee joints induces osteoarthritis in mice. *Osteoarthritis Cartilage* 2013;21:491-97.
41. van der Kraan PM and van den Berg WB. Chondrocyte hypertrophy and osteoarthritis: role in initiation and progression of cartilage degeneration? *Osteoarthritis Cartilage* 2012;20:223-32.
42. Demidenko ZN and Blagosklonny MV. Growth stimulation leads to cellular senescence when the cell cycle is blocked. *Cell Cycle* 2008;7:3355-61.
43. Philipot D, Guerit D, Platano D, Chuchana P, Olivotto E, Espinoza F, et al. p16INK4a and its regulator miR-24 link senescence and chondrocyte terminal differentiation-associated matrix remodeling in osteoarthritis. *Arthritis Res Ther* 2014;16:R58.
44. Guidotti S, Minguzzi M, Platano D, Cattini L, Trisolino G, Mariani E, et al. Lithium Chloride Dependent Glycogen Synthase Kinase 3 Inactivation Links Oxidative DNA Damage, Hypertrophy and Senescence in Human Articular Chondrocytes and Reproduces Chondrocyte Phenotype of Obese Osteoarthritis Patients. *PLoS One* 2015;10:e0143865.
45. Takacs-Buia L, Iordachel C, Efimov N, Caloianu M, Montreuil J and Bratosin D. Pathogenesis of osteoarthritis: chondrocyte replicative senescence or apoptosis? *Cytometry B Clin Cytom* 2008;74:356-62.
46. Sommaggio R, Perez-Cruz M, Brokaw JL, Manez R and Costa C. Inhibition of complement component C5 protects porcine chondrocytes from xenogeneic rejection. *Osteoarthritis Cartilage* 2013;21:1958-67.
47. Xie LS and Huang YJ. Antagonism of RIP1 using necrostatin-1 (Nec-1) ameliorated damage and inflammation of HBV X protein (HBx) in human normal hepatocytes. *Artif Cell Nanomed B* 2019;47:1194-99.

Figure 1: Schematic illustration of the current concept of complement involvement in cartilage damage and degeneration after trauma. Cartilage trauma and subsequent release of DAMPs triggers activation of the complement cascade and oxidative stress. Cleavage of the central factor C3 generates anaphylatoxin C3a and C3b, a component of the C5-convertase PC3bBbC3b, which can be inhibited by ATA. Subsequent cleavage of C5 into C5a (another anaphylatoxin) and C5b initiates C5b-9 formation. While CLU specifically binds to TCC-components C7, C8 and C9, ATA inhibits the polymerization of C9 to the C5b-8 complex. Integration of the TCC into the plasma membrane leads to cell death signaling, including apoptosis and necroptosis, as well as expression of hypertrophy and senescence markers in chondrocytes. Downstream signaling of the TCC can be differentially modulated by the antioxidant NAC, RIPK-1 inhibitor Nec-1 and pan-caspase inhibitor zVAD.
Abbreviations: ATA = aurintricarboxylic acid, COL10A1 = type X collagen (alpha 1 chain), MMP-13 = matrix metalloproteinase 13, CXCL1 = chemokine (C-X-C motif) ligand 1, DAMPs = damage-associated molecular pattern, IL-6/-8 = interleukin 6/ 8, NAC = N-acetyl cysteine, Nec-1 = Necrostatin-1, ROS/RNS = reactive oxygen/nitrogen species, PC3bBb = properdin-C3b-Factor B complex, zVAD = z-VAD-FMK.

Figure 2: TCC deposition and endogenous inhibitors in native osteoarthritic cartilage and *ex vivo* tissue culture. IHC staining of membrane-bound TCC and gene expression of complement regulators CD59 and CLU were determined in (**A,E**) highly degenerated cartilage tissue (ICRS grade ≥ 3; n=8) as well as (**C,F,G**) *ex vivo* traumatized and HS-stimulated macroscopically intact cartilage (ICRS grade ≤ 1; n ≥4). (**B**) Unimpacted cartilage (ICRS grade ≤ 1) served as control; (**D**) IgG isotype control; gray filled bars = OA tissue, blank bars = unimpacted control; black patterned bars = traumatized; striped bars = traumatized and exposed to HS; hi = heat-inactivated human serum (HS). Bars in the IHC images represent 100 µm. Significant differences between groups were depicted as: ** $p < 0.01$, ****$p \leq 0.0001$. Significant differences vs C were depicted as: ^{C} $p < 0.05$, ^{CC} $p < 0.01$, ^{CCCC} $p \leq 0.0001$.

Figure 3: Effects of HS and cartilage trauma on cell viability and gene expression of necroptotic and apoptotic markers. Traumatized cartilage explants were exposed to different concentrations of HS (10-30% v/v). (**A**) Cytotoxicity was evaluated by live dead staining and gene expression of necroptosis- ((**B**) RIPK1, (**C**) RIPK3 and (**D**) MLKL) and apoptosis-related ((**E**) CASP3, (**F**) CASP8) proteins was determined. Unimpacted cartilage explants served as control; n ≥4. Blank bars = unimpacted control (C); black patterned bars = traumatized; striped bars = traumatized and exposed to HS; hi = heat-inactivated human serum (HS). Significant differences between groups were depicted as: * $p < 0.05$, ** $p < 0.01$. Significant differences vs C were depicted as: ^{CC} $p < 0.01$, ^{CCC} < 0.001, ^{CCCC} $p \leq 0.0001$.

Figure 4: Evaluation of potential triggers and inhibitors of TCC formation. (**A**) TCC deposition on isolated chondrocytes was quantified by a specific C5b-9 cell-ELISA. Values are given in relation to the levels of the serum-free (SF) control; n ≥ 4. blank bars = no additional HG/ TCM as trigger included; black patterned bar = trauma-conditioned medium (TCM) added; striped bars = HG added; hi = heat-inactivated human serum (HS), HG = homogenized cartilage; z = zVAD. Significant differences between groups were depicted as: * $p < 0.05$, ** $p < 0.01$, *** $p < 0.001$, **** $p < 0.0001$. Significant differences vs SF were depicted as: $^{\#}$ $p < 0.05$, $^{\#\#\#\#}$ $p \leq 0.0001$. (**B**) Hemolytic activity of the serum w/ and w/o addition of different therapeutics was determined by a CH-50 assay (n ≥ 2); TBS control = no HS added (zero value), HS control = no treatment applied.

Figure 5: Effects of therapeutic treatment on serum-mediated regulated cell death after cartilage trauma. Traumatized cartilage explants were exposed to HS (30% v/v) and cartilage homogenate (HG; 20 µg/mL). (**A**) Cytotoxicity was evaluated by live dead staining and gene expression of necroptosis- ((**B**) RIPK1, (**C**) RIPK3 and (**D**) MLKL) and apoptosis-related ((**E**) CASP3, (**F**) CASP8) proteins was determined. Additionally, different therapeutics were tested: NAC (2 mM), Nec (40 µM), NSA (2.5 µM), zVAD (z; 20 µM), ATA (75 µg/mL)

and CLU (30 µg/mL). Unimpacted cartilage explants served as control (C); n ≥5. Blank bars = unimpacted control; striped bars = traumatized and exposed to HS; hi = heat-inactivated human serum (HS). Significant differences between groups were depicted as: * $p < 0.05$, ** $p < 0.01$, *** $p < 0.001$, **** $p < 0.0001$. Significant differences vs C were depicted as: $^{###}$ $p < 0.001$, $^{####}$ $p \leq 0.0001$. Significant differences vs T were depicted as: ^{ttt} $p < 0.001$.

Figure 6: Effects of HS and therapeutic treatment on the gene expression of hypertrophy and senescence markers after cartilage trauma. Traumatized cartilage explants were exposed to HS (30% v/v) and cartilage homogenate (HG; 20 µg/mL). Phenotypical changes were assessed by gene expression analysis of hypertrophy- and senescence-associated markers ((**A**) COL10A1, (**B**) MMP-13, (**C**) CXCL1, (**D**) IL-8, (**E**) RUNX2 and (**F**) VEGFA). Additionally, different therapeutics were tested: NAC (2 mM), Nec (40 µM), zVAD (z; 20 µM), ATA (75 µg/mL) and CLU (30 µg/mL). Unimpacted cartilage explants served as control (C); n ≥5. Significant differences between groups were depicted as: * $p < 0.05$, ** $p < 0.01$, *** $p < 0.001$, **** $p < 0.0001$. Significant differences vs C were depicted as: ^{CCC} $p < 0.001$. Blank bars = unimpacted cartilage, black patterned bars = traumatized cartilage, striped bars = impacted and serum-/ HG-stimulated cartilage; hi = heat-inactivated human serum (HS).

Figure 7: Effects of HS and therapeutic treatment on SA-ß-galactosidase activity and secretion of hypertrophy and senescence markers after cartilage trauma. Traumatized cartilage explants were exposed to HS (30% v/v) and cartilage homogenate (HG; 20 µg/mL). Phenotypical changes were assessed by secretion of hypertrophy- and senescence-associated markers (**A**) MMP-13 and (**B**) IL-6. Additionally, different therapeutics were tested: NAC (2 mM), Nec (40 µM), zVAD (z; 20 µM), ATA (75 µg/mL) and CLU (30 µg/mL). (**C**) SA-ß-galactosidase (gal) was determined in isolated chondrocytes in different passages stimulated with HS (30% v/v) and HG for 48 h. (D) Quantification of SA-ß-gal-positive cells. Unimpacted cartilage explants served as control (C); n ≥5. Significant differences between

groups were depicted as: * $p < 0.05$, *** $p < 0.001$, **** $p < 0.0001$. Significant differences vs C were depicted as: ^{C} $p < 0.05$, ^{CC} $p < 0.01$, ^{CCC} $p < 0.001$, ^{CCCC} $p \leq 0.0001$. Blank bars = unimpacted cartilage, black patterned bars = traumatized cartilage, striped bars = impacted and serum-/ HG-stimulated cartilage; hi = heat-inactivated human serum (HS)/ fetal calf serum (FCS).

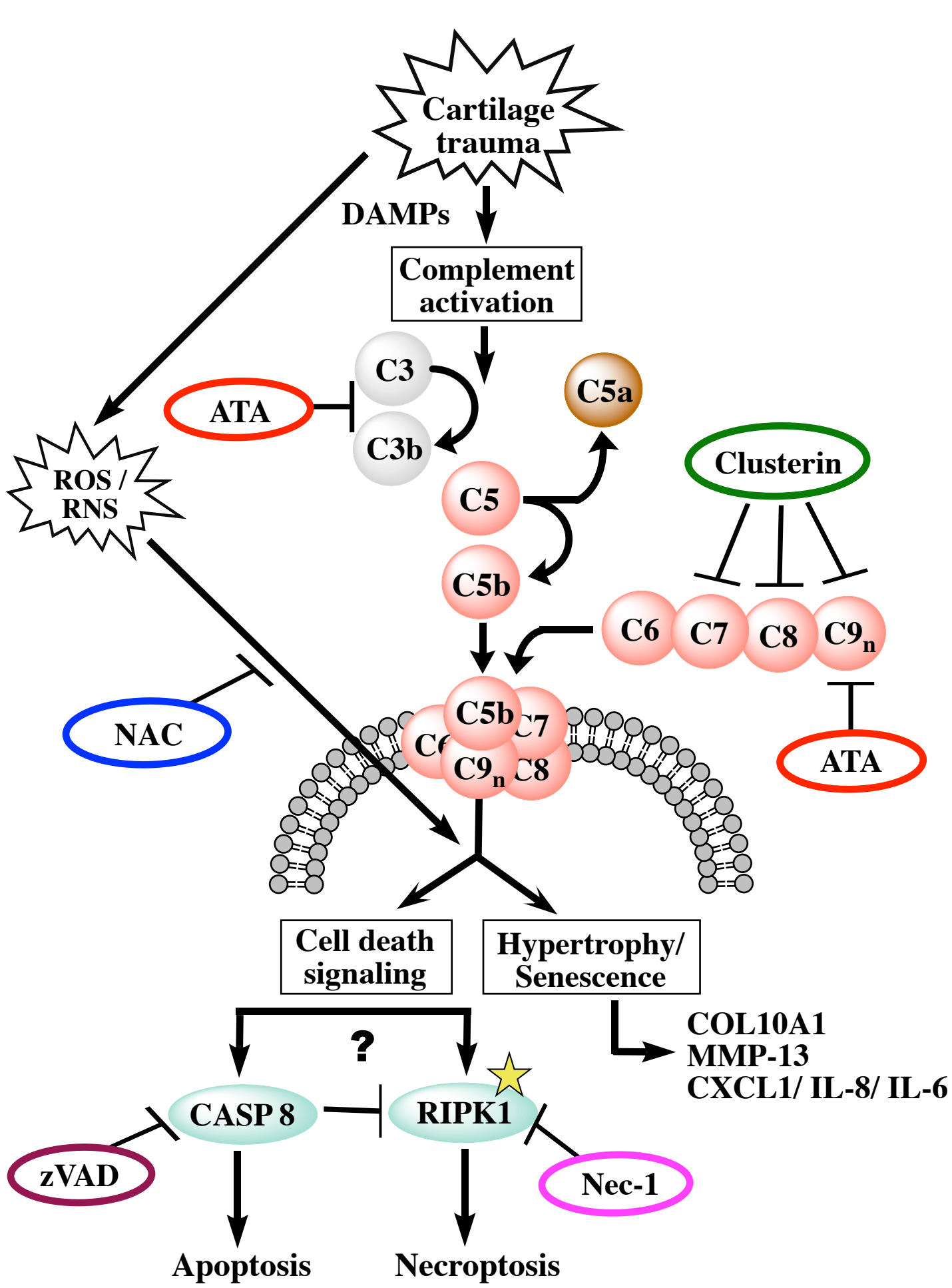
Cartilage trauma
DAMPs
Complement activation
C3
C3b
ATA
C5a
C5
C5b
ROS / RNS
Clusterin
C6
C7
C8
C9n
ATA
NAC
C5b
C7
C6
C9n
C8
Cell death signaling
Hypertrophy/ Senescence
COL10A1
MMP-13
CXCL1/ IL-8/ IL-6
?
CASP 8
RIPK1
zVAD
Nec-1
Apoptosis
Necroptosis

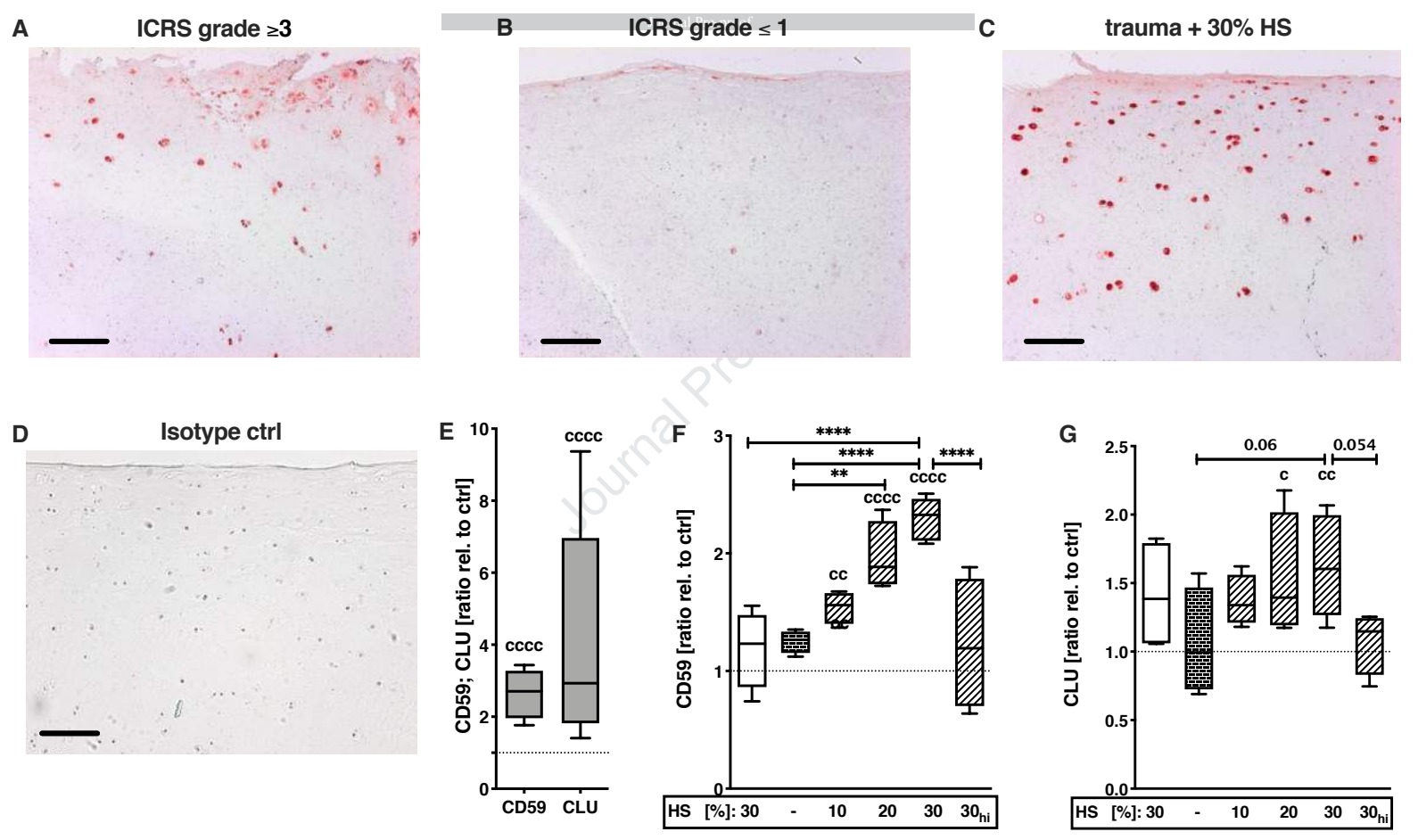
A
ICRS grade ≥3
B
ICRS grade ≤ 1
C
trauma + 30% HS
D
Isotype ctrl
E
CD59; CLU [ratio rel. to ctrl]
cccc
cccc
CD59
CLU
F
CD59 [ratio rel. to ctrl]
****
****
**
****
cc
cccc
cccc
HS [%]: 30 - 10 20 30 30hi
G
CLU [ratio rel. to ctrl]
0.06
0.054
c
cc
HS [%]: 30 - 10 20 30 30hi